BVRI light curves, period and spectroscopic study of a low mass-ratio contact binary HV Aqr

Ahmed Waqas Zubairi[a,b,c,d], Zhou Xiao[a,c,d], Eduardo Fernȼndez Lajs[e,f], Zhu Liying[a,b,c,d], Liao Wenping[a,b,c,d], Soonthornthum Boonrucksar[g], Zhang Bin[h], Sarotsakulchai Nopphadon[g]

[a] *Yunnan Observatories, Chinese Academy of Sciences, Kunming 650216, China*
[b] *University of Chinese Academy of Sciences, Yuquan Road 19, Sijingshang Block, 100049 Beijing, China*
[c] *Center for Astronomical Mega-Science, Chinese Academy of Sciences, Beijing 100101, China*
[d] *Key Laboratory of the Structure and Evolution of Celestial Objects, Chinese Academy of Sciences, P.O. Box 110, 650216 Kunming, China*
[e] *Facultad de Ciencias Astronmicas y Geofsicas, Universidad Nacional de La Plata, 1900 La Plata, Buenos Aires, Argentina*
[f] *Instituto de Astroflsica de La Plata (CCT La plata - CONICET/UNLP), Argentina*
[g] *National Astronomical Research Institute of Thailand, 260 Moo 4, T. Donkaew, A. Maerim, Chiangmai, 50180, Thailand*
[h] *School of Physics and Electronic Science, Guizhou Normal University, 550001 Guiyang, China*

Abstract

New BVRI light curves of the short period binary system, HV Aqr, are presented. Photometric solutions were derived using the 2015 version of WilsonCDevinney code. The complete eclipses of the light curves of HV Aqr enable us to determine high-precision photometric parameters of the binary system. The new solution suggest that HV Aqr is a low mass ratio ($q = 0.145$) deep contact binary with a contact degree of $f = 74.19\%$. Based on all available times of light minimum, we analyzed the long-term period changes of HV Aqr. A decrease rate of $dP/dt = -9.01 \times 10^{-8} days/yr$ was determined. The continuous period decrease can be explained by the mass transfer from the primary component to the secondary and angular momentum loss via magnetic stellar wind. A conservative mass transfer rate of $1.876 \times 10^{-8} M_{\odot} yr^{-1}$ and angular momentum loss rate at $6.25 \times 10^{39} Kg\, m^2\, s^{-1}\, yr^{-1}$ were derived. As the orbital period decreases, the contact degree of HV Aqr will become deeper and finally it will evolve into a single rapid-rotating star.

Keywords: binaries: eclipsing – binaries: spectroscopic – stellar: evolution – individual: HV Aqr.

1. Introduction

HV Aqr is considered as an extreme low-mass ratio contact binary system and was first observed by Schirmer & Geyer (1992) with $q = 0.146$ and $f = 47.5\%$ having the orbital period of 0.374479 days. Further investigations showed that system has $P = 0.37445764$ days. Rucinski et al. (2000) derived a mass ratio $q = 0.145 \pm 0.050$ and F5V spectral type according to their radial velocity measurements study. His published mass ratio and fill-out factor were slightly different from previous observations of Molik & Wolf (2000). They reported $q = 0.18$ and $f = 40\%$. Later on, D'Angelo et al. (2006) found the signature of a tertiary component and identified HV Aqr as a triple system. Gazeas et al. (2007) obtained larger degree of contact ($f = 68.3\%$) and the mass ratio $q = 0.151$ in a presence of O'Connell effect (O'Connell, 1951). In 2013, Li & Qian (2013) analysis of *VRI* light curves showed $q = 0.1455$ and $f = 55.9\%$. They derived the period of $P = 0.37445838$ days which is decreasing at the rate of $dP/dt = 8.84 \times 10^{-8} days/yr$. More recently, Gazeas et al. (2021) modeled the light curve of HV Aqr with negligible third light with $q = 0.140$ and $f = 74\%$. It was proposed that system may further be observed to study the period and light curve.

In this paper, we presented the new BVRI light curves of HV Aqr. Using the 2015 version of Wilson-Devinney code, new photometric solutions of the system were obtained. We analyzed the long-term orbital period variation of HV Aqr based on all available times of light minimum. In addition to that, the spectroscopic observations helped us understanding the properties of HV Aqr.

*Corresponding author: zhouxiaophy@ynao.ac.cn (X. Zhou)

2. Observation of HV Aqr

2.1. Spectroscopic Data

The low-resolution spectrum of HV Aqr was obtained using 2.4m optical telescope at Lijiang observational station of Yunnan Observatories. The Yunnan Faint Object Spectrograph and Camera (YFOSC) is used to obtain low-resolution spectrum. The CCD for YFOSC is a 2148×4612 pixel with the pixel size of $13.5\mu m \times 13.5\mu m$. The data was obtained using slit size of $168\mu m$ at resolution of $3520nm/pix$. The target was observed for two consecutive nights on October 24-25, 2021 with an exposure time of 900 seconds. The obtained spectrum is shown in Figure 1. The atmospheric parameters and probable errors are shown in Table 1. These parameter were obtained using the Universite de Lyon spectroscopic analysis software (ULySS) (Koleva et al., 2009; Wu et al., 2011). This is the same method as used for LAMOST data (Wu et al., 2011).

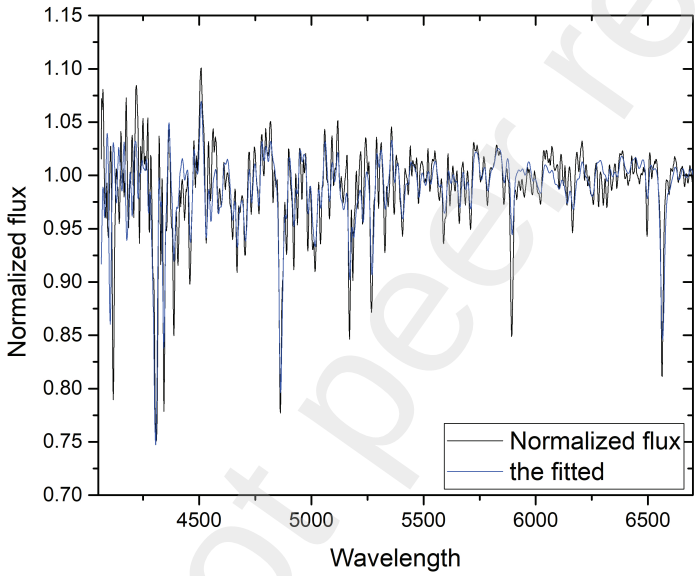

Figure 1: The black line shows the low-resolution spectrum of HV Aqr which is fitted over the LAMOST spectrum (blue line). The wavelength is in angstrom.

Table 1: Atmospheric parameter of HV Aqr

HJD	$T_{eff}(K)$	$log(g)(cm/s^2)$	$[Fe/H](dex)$
2459512.08	5873.244 ± 33.31	3.527 ± 0.105	0.107 ± 0.052
2459513.125	5958.406 ± 29.12	3.662 ± 0.094	0.104 ± 0.047

2.2. Photometric Observations

The photometric data is obtained with 0.6m Helen Sawyer Hogg (HSH) telescope located at Complejo Astronomico El Leoncito (CASLEO), San Juan, Argentina. The telescope is equipped with SBIG STL1001E CCD camera with standard Jhonson's BVRI filters. The observing equipment provides a good field of view of 9.3×9.3 arc minutes in 1×1 binning. The HV Aqr was observed on August 02, 2019 and complete light curves were obtained in all BVRI filters. The exposure time was 10-20 seconds. Table 2 represents GCVS catalog numbers, coordinates and BVRI magnitudes of HV Aqr, comparison star C1 and check star C2. The new determined times of primary and secondary minimum are listed in Table 3.

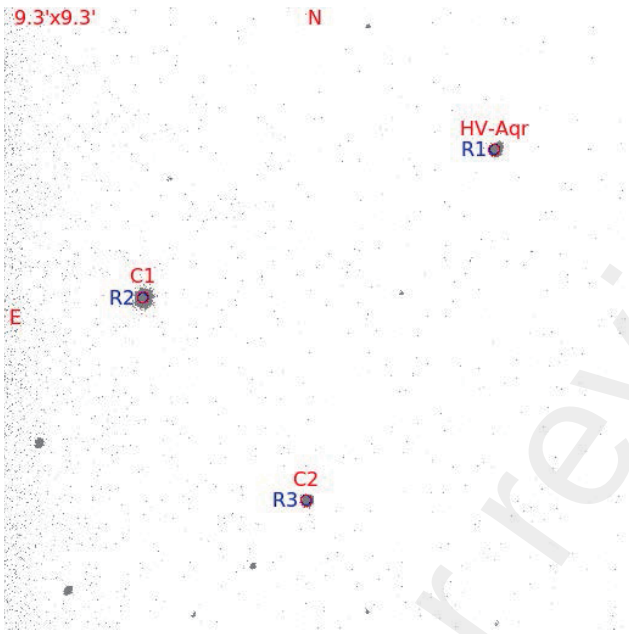

Figure 2: The 9.3×9.3 arc minutes field of view from our observing equipment at HSH-CASLEO. The comparison and check stars also marked as C1 and C2, respectively.

Table 2: Coordinates and magnitudes of HV Aqr, its comparison star and check star

System	α(2000)	δ(2000)	B	V	R	I
HV Aqr (GSC 05198-00659)	21 21 24.81	-03 09 36.84	10.50	9.99	-	9.15
C1 (GSC 05198-01308)	21 21 46.49	-03 11 57.72	9.60	8.40	-	-
C2 (GSC 05198-00636)	21 21 36.30	-03 15 04.93	9.60	8.40	-	-

3. Orbital Period Study

We obtained total 99 times of primary and secondary minima for our analysis including the present observations. Most of the minima data is available at O-C gateway ($http://var2.astro.cz/ocgate$) and Bob Nelson files ($https://www.aavso.org/bob-nelsons-o-c-files$). The O-C diagram indicates parabolic fit as shown in the Figure 3. The least square method yields that period of HV Aqr is decreasing. We obtained the new ephemeris and period of HV Aqr.

$$MinI = 2458697.8505(2) + 0.37445590(5)E - 4.62(9) \times 10^{-11}E^2 \quad (1)$$

The quadratic term in Equation 1 leads us to determine the period decrease rate of $dP/dt = -9.01 \times 10^{-8} days/yr$.

Table 3: New times of light minimum for HV Aqr.

HJD	Error	Filter	Type
2458697.8510	±0.0002	B	I
2458697.8510	±0.0002	V	I
2458697.8507	±0.0002	R	I
2458697.8513	±0.0002	I	I
2458697.6638	±0.0002	B	II
2458697.6636	±0.0002	V	II
2458697.6633	±0.0001	R	II
2458697.6640	±0.0002	I	II

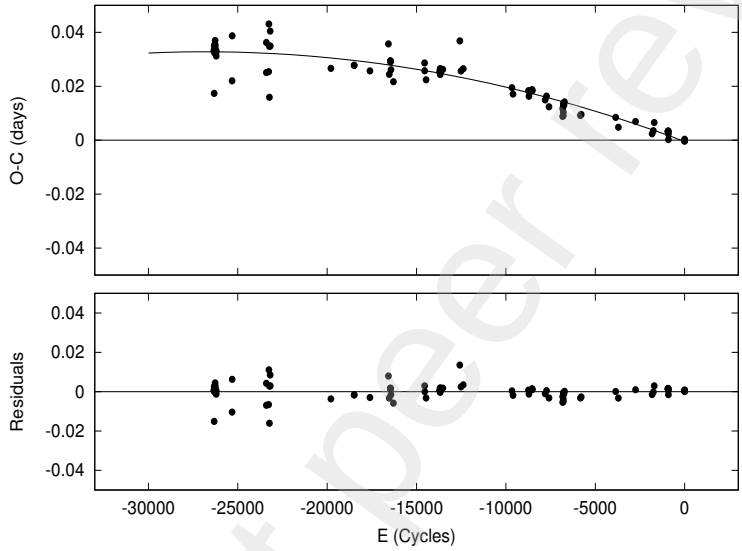

Figure 3: O-C diagram of HV Aqr. Circles represents all times of primary and secondary minima. Black line shows parabolic fit. Residuals are plotted in the bottom panel.

4. Light Curve Analysis

The simultaneous BVRI solution for HV Aqr is obtained using 2015 version of the Wilson-Devinney program (WD) (Wilson & Devinney, 1971; Wilson & Van Hamme, 2014). The gravity darkening coefficients (g_1, g_2) and albedo (A_1, A_2) were set to 0.32 and 0.5 respectively as these values are reasonable for stars having convective envelopes (Lucy, 1967; Ruciński, 1969). The square root limb darkening parameter (x_1, x_2, y_1, y_2) were obtained from van Hamme (1993). The spectroscopic mass ratio ($q = 0.145$) of (Rucinski et al., 2000) was used and kept fixed. The average temperature of star 1 (T_1) was used from our low resolution spectrum listed in Table 1. The orbital inclination (i), temperature of star 2 (T_2), the dimensionless gravitational potential (Ω_1) (for contact binaries $\Omega_1 = \Omega_2$), and the luminosity of star 1 (L_1), were kept adjustable. All adjustable parameters converged properly. However, significant difference in amplitude was observed in the light curve especially in BVR filters. Initially, we added a cool spot which improved the light curve mostly at outside the minimas. However, the difference in amplitude of light curve remained. We, therefore, offer a single hot spot which significantly improved the light curves fit. The solution converged properly with an improved mean residual. The results are tabulated in Table 7. We found that spot solution showed a better and improved value of mean residual. We adopted spot solution and super imposed the modeled light curve over the observed as shown in Figure 4.

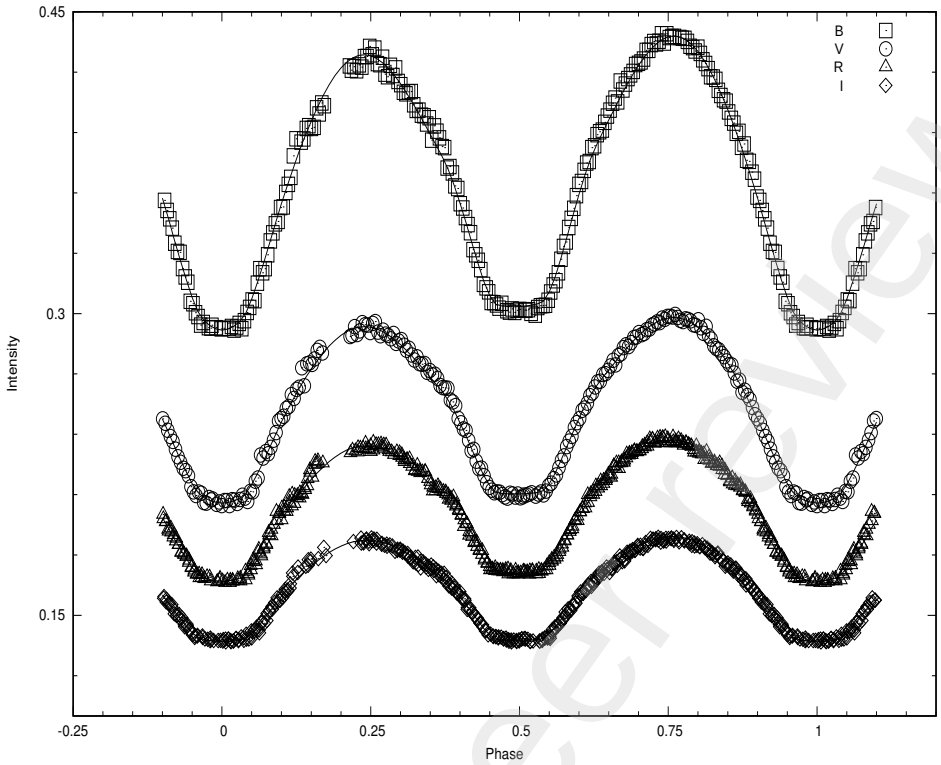

Figure 4: Combined light curves of HV Aqr in BVRI filters. The solution (solid line) is superimposed over observed light curve.

5. Spot Activity

The movement of spots on either or both components of a binary system along with the rotation of each star make the study of spot activity on eclipsing binaries more complicated (Sarotsakulchai et al., 2019; Xia et al., 2021). According to the photometric solution of Gazeas et al. (2007), HV Aqr showed the O'Connell effect in the light curves which he explained with a small cool spot with radius of 17 degree. Later on, Gazeas et al. (2021) introduced 31 degrees large cool spot. The latitude of both spots were different, however, they were almost at the same longitudinal position and the later was relatively at lower temperature. The present study indicates that HV Aqr is having a hot spot of 22 degrees radius. The latitude and longitudinal positions are also different compared to previously reported spots. Table 4 list the values of spot parameters. A simple unit conversion makes the values consistent.

Table 4: Star spot parameters for HV Aqr

Parameters	Gazeas et al. (2007)	Gazeas et al. (2021)	Present study
Latitude(deg)	65.6	151	117.45
Longitude (deg)	32.1	33	96.19
Angular Radius (deg)	17.3	30.7	22.05
Spot Temp. Factor	0.945	0.89	1.05

6. Results and Discussion

The asymmetries in light curve were first reported by Schirmer & Geyer (1992) and Robb (1992). However, Molik & Wolf (2000) and Li & Qian (2013) presented symmetric light curves. Rucinski et al. (2007) found a tertiary

component with HV Aqr. Gazeas et al. (2007, 2021) suggested the presence of O'Connell effect (Max. II fainter than Max. I) and introduced a cool spot on either component. They also presented the third light solution of the system. However, we did not find any third light in our solution.

In our new determined BVRI light curves, we observed that Max. I is fainter than Max. II. This can easily be noticed particularly in B-light curve. We calculated the Max. I − Max. II values of the light curves and list in Table 5. This indicates that HV Aqr is going through a cycle of magnetic activity and can be a hot spot on either component.

Table 5: Table of Max. I-II values for observed HV Aqr light curve

Filter	Max. I-II	Reference
B	0.035	Present study
V	0.024	Present study
	-0.019	Robb (1992)
	0.013	Gazeas et al. (2007)
	-0.003	Li & Qian (2013)
R	0.019	Present study
	-0.015	Robb (1992)
	0.012	Gazeas et al. (2007)
	-0.004	Li & Qian (2013)
I	0.007	Present study

The variation in Max. I-II values and the spot parameters shows that the O'Connell effect is variable. This also shows two types of activity scenarios. We call it the active scenario when Max I ≠ Max II and inactive scenario when Max I = Max II (Qian et al., 2014). Since data points are not sufficient to determine the Max. I-II activity, therefore, we recommend continuous and long term monitoring of light curve.

A small mass ratio along with high value of orbital inclination produces a total eclipse with fully obscured less massive component. Such situation allows to determine accurate parameters of the system(Li et al., 2019, 2021). Using radial velocity data of Rucinski et al. (2000) and our present photometric solution, we have derived the absolute parameters for HV Aqr. These are listed in Table 6.

Table 6: Absolute parameters for *HVAqr*

Parameter	Value
a	$2.540 R_\odot \pm 0.187$
M_1	$1.379 M_\odot \pm 0.388$
M_2	$0.200 M_\odot \pm 0.388$
R_1	$1.466 R_\odot \pm 0.073$
R_2	$0.673 R_\odot \pm 0.073$
L_1	$2.351 L_\odot \pm 0.102$
L_2	$0.512 L_\odot \pm 0.217$

The period study shows that HV Aqr is going through period decrease at $9.01 \times 10^{-8} days/yr$. This can be explained through evolutionary scenario of thermal relaxation oscillation with Angular Momentum Loss (AML) via change in degree of contact (Lucy, 1976; Flannery, 1976; Robertson & Eggleton, 1977; Qian, 2003). This suggests that evolution of HV Aqr is controlled by AML. The continuous decrease in period also suggests that HV Aqr is undergoing a process of mass transfer from primary to secondary component. We can use the well-known equation (Carroll & Ostlie, 2017)

$$\frac{dP/dt}{P} = -3\,\frac{dM_1}{dt}\left(\frac{1}{M_1} - \frac{1}{M_2}\right) \tag{2}$$

to determined the mass transfer rate of $1.876 \times 10^{-8} M_{\odot} yr^{-1}$ at a time scale ($t = \frac{M_1}{dM_1/dt}$) of $7.35 \times 10^7\ yr$. The thermal time scale ($\frac{GM^2}{RL}$) (Karttunen et al., 2007) of secondary component is $3.58 \times 10^6\ yr$. The strong magnetic activity and decrease in period caused by AML,

$$\frac{dJ}{dt} = \frac{G}{6\pi} \frac{M_1^2 a^2}{R_2^3} \frac{dP}{dt} \tag{3}$$

Using Equation 3, we have determine the angular momentum loss rate at $6.25 \times 10^{39} Kg\, m^2\, s^{-1}\, yr^{-1}$. The continuous decrease in period is not only because of mass transfer from primary to secondary component but also from AML. The cyclic variation in period cannot be determined because of insufficient data on light minima. The large fill-out factor shows that HV Aqr is in deep contact configuration. With the decrease in orbital period, the inner and outer Roche lobes will shrink which causes the common convective envelope to become deeper. The process will continue until the formation of single, rapid-rotating star is formed.

Acknowledgements

This research was supported by the National Natural Science Foundation of China (Grant No. 11933008 and 11873017), the Joint Research Fund in Astronomy (Grant No. U1931101) under cooperative agreement between the National Natural Science Foundation of China and Chinese Academy of Sciences and the basic research project of Yunnan Province (Grant No. 202201AT070092). This research has made use of the SIMBAD database, operated at CDS, Strasbourg, France. The work is jointly supported by the Chinese Academy of Sciences (CAS) and the World Academy of Sciences (TWAS).

References

Carroll, B. W. & Ostlie, D. A. 2017, An introduction to modern astrophysics, Second Edition, by Carroll, Bradley W.; Ostlie, Dale A., 2017. Cambridge: Cambridge University Press. OCLC: 991641816. ISBN: 9781108422161.

D'Angelo, C., van Kerkwijk, M. H., & Rucinski, S. M. 2006, AJ, 132, 650. doi:10.1086/505265

Flannery, B. P. 1976, ApJ, 205, 217. doi:10.1086/154266

Gazeas, K. D., Niarchos, P. G., & Zola, S. 2007, Solar and Stellar Physics Through Eclipses, 370, 279

Gazeas, K., Zola, S., Liakos, A., et al. 2021, MNRAS, 501, 2897. doi:10.1093/mnras/staa3753

Koleva, M., Prugniel, P., Bouchard, A., et al. 2009, A&A, 501, 1269. doi:10.1051/0004-6361/200811467

Karttunen, H., Krüger, P., Oja, H., et al. 2007, Fundamental Astronomy

Li, K. & Qian, S.-B. 2013, NewA, 21, 46. doi:10.1016/j.newast.2012.11.003

Li, K., Xia, Q.-Q., Liu, J.-Z., et al. 2019, Research in Astronomy and Astrophysics, 19, 147. doi:10.1088/1674-4527/19/10/147

Li, K., Xia, Q.-Q., Kim, C.-H., et al. 2021, AJ, 162, 13. doi:10.3847/1538-3881/abfc53

Lucy, L. B. 1967, ZA, 65, 89

Lucy, L. B. 1976, ApJ, 205, 208. doi:10.1086/154265

Molik, P. & Wolf, M. 2000, Information Bulletin on Variable Stars, 4951, 1

O'Connell, D. J. K. 1951, Publications of the Riverview College Observatory, 2, 85

Qian, S. 2003, MNRAS, 342, 1260. doi:10.1046/j.1365-8711.2003.06627.x

Qian, S.-B., Wang, J.-J., Zhu, L.-Y., et al. 2014, ApJS, 212, 4. doi:10.1088/0067-0049/212/1/4

Robb, R. M. 1992, Information Bulletin on Variable Stars, 3798, 1

Robertson, J. A. & Eggleton, P. P. 1977, MNRAS, 179, 359. doi:10.1093/mnras/179.3.359

Ruciński, S. M. 1969, AcA, 19, 245

Rucinski, S. M., Lu, W., & Mochnacki, S. W. 2000, AJ, 120, 1133. doi:10.1086/301458

Rucinski, S. M., Pribulla, T., & van Kerkwijk, M. H. 2007, AJ, 134, 2353. doi:10.1086/523353

Sarotsakulchai, T., Qian, S.-B., Soonthornthum, B., et al. 2019, PASJ, 71, 81. doi:10.1093/pasj/psz062

Schirmer, J. & Geyer, E. H. 1992, Information Bulletin on Variable Stars, 3785, 1

van Hamme, W. 1993, AJ, 106, 2096. doi:10.1086/116788

Wilson, R. E. & Devinney, E. J. 1971, ApJ, 166, 605. doi:10.1086/150986

Wilson, R. E. & Van Hamme, W. 2014, ApJ, 780, 151. doi:10.1088/0004-637X/780/2/151

Wu, Y., Singh, H. P., Prugniel, P., et al. 2011, A&A, 525, A71. doi:10.1051/0004-6361/201015014

Wu, Y., Luo, A.-L., Li, H.-N., et al. 2011, Research in Astronomy and Astrophysics, 11, 924. doi:10.1088/1674-4527/11/8/006

Xia, Q., Michel, R., Li, K., et al. 2021, PASP, 133, 054202. doi:10.1088/1538-3873/abf32d

Table 7: Photometric solution for HV Aqr

Parameters	No Spot	Spot
$q(m_2/m_1)^1$	0.145	0.145
$i(deg)$	79.24 ± 0.29	77.60 ± 0.29
$\Omega_1 = \Omega_2$	2.022 ± 0.001	2.020 ± 0.001
Ω^1_{in}	2.089	2.089
Ω^1_{out}	1.996	1.996
$T^1_1(K)$	5915	5915
$T_2(K)$	5970 ± 9	5963 ± 8
$x_{1B,2B}$	0.453, 0.385	0.453, 0.385
$x_{1V,2V}$	0.210, 0.050	0.210, 0.050
$x_{1R,2R}$	0.084, 0.022	0.084, 0.022
$x_{1I,2I}$	-0.061, -0.190	-0.061, -0.190
$y_{1B,2B}$	0.422, 0.489	0.422, 0.489
$y_{1V,2V}$	0.633, 0.652	0.633, 0.652
$y_{1R,2R}$	0.678, 0.693	0.678, 0.693
$y_{1I,2I}$	0.687, 0.668	0.687, 0.668
$A^1_{1,2}$	0.50	0.50
$g^1_{1,2}$	0.32	0.32
$L_1/(L_1 + L_2)_B$	0.826 ± 0.001	0.827 ± 0.001
$L_1/(L_1 + L_2)_V$	0.821 ± 0.001	0.822 ± 0.001
$L_1/(L_1 + L_2)_R$	0.828 ± 0.001	0.828 ± 0.001
$L_1/(L_1 + L_2)_I$	0.825 ± 0.001	0.825 ± 0.001
$r_1(pole)$	0.5282 ± 0.0003	0.5283 ± 0.0003
$r_1(side)$	0.5889 ± 0.0006	0.5892 ± 0.0005
$r_1(back)$	0.6150 ± 0.0007	0.6153 ± 0.0006
$r_2(pole)$	0.2335 ± 0.0004	0.2340 ± 0.0004
$r_2(side)$	0.2461 ± 0.0005	0.2468 ± 0.0005
$r_2(back)$	0.3119 ± 0.0019	0.3141 ± 0.0018
Latitude(rad)[1]	-	2.050
Longitude (rad)	-	1.679 ± 0.039
Angular Radius (rad)	-	0.385 ± 0.010
Spot Temp. Factor[1]	-	1.050
$f(\%\, of\, overflow)$	72.04%	74.19%
Mean Residual	0.0003084	0.0003073

[1]Fixed Values